Compressible metamagnetic model: Renormalization-group approach

A. F. S. Moreira,[1] W. Figueiredo,[1,2] and V. B. Henriques[3]
[1]*Departamento de Física, Universidade Federal de Santa Catarina, 88040-900 Florianópolis, Santa Catarina, Brazil*
[2]*H. H. Wills Physics Laboratory, Royal Fort, Tyndall Avenue, Bristol BS8 1TL, United Kingdom*
[3]*Instituto de Física, Universidade de São Paulo, Caixa Postal 66318, 05389-970 São Paulo, Brazil*
(Received 8 March 2007; published 28 June 2007)

A layered compressible metamagnetic Ising model is studied within the renormalization-group approach. The ferro- and antiferromagnetic couplings depend linearly on volume, so shear forces are infinite, as in Domb's compressible ferromagnetic model [J. Chem. Phys. **25**, 783 (1956)]. The Hamiltonian is expanded around the mean-field solution and the resulting functional contains both the biquadratic term, characteristic of compressibility, and the rigid metamagnetic characteristic cubic terms. However, a different contribution, related to the anisotropy of the spin-lattice coupling, arises. Mean-field behavior is reproduced only partially. However, differently from the infinite-shear compressible ferromagnetic case, some of the fixed points can be accessed within the physical domain of the variables, for some range of the interaction parameters. In this case, the continuous transition line at intermediate magnetic fields presents Fisher-renormalized critical exponents [Phys. Rev. **176**, 257 (1968)]. The two tricritical points present Ising exponents (at low field) and Fisher-renormalized Gaussian exponents.

DOI: 10.1103/PhysRevB.75.224432 PACS number(s): 05.70.Fh, 05.70.Jk, 05.10.Cc

I. INTRODUCTION

A metamagnetic system can be viewed as a stacking of identical spin layers with only nearest neighbor interactions, ferromagnetic inside and antiferromagnetic between adjacent layers. Metamagnets have been studied in the literature both theoretically[1–9] and experimentally.[10–12] In general, their phase diagram exhibit first-order paramagnetic-antiferromagnetic transitions at high magnetic fields and a line of continuous transitions at low fields. The two lines usually join at a tricritical point, but some theoretical investigations allow more complex behaviors.

Compressibility of ferromagnetic Ising systems was addressed in a series of theoretical studies[13–21] some time ago. For an exchange interaction linearly dependent on inter-ion distance, integration of elastic variables leads to effective long-range four-spin interaction. Two simple limiting cases correspond to infinite[13] and zero[14] shear forces. Finite shear was also the subject of investigation in Refs. 16 and 20. For the shearless Baker-Essam model,[14] both the elastic and magnetic couplings depend only on the longitudinal component of the relative positions of the ions. It presents Ising critical indices under constant pressure and Ising renormalized critical indices at constant volume.[14,19] In Domb's compressible[13] model, position fluctuations are absent and inter-ion distances are only volume dependent. Mean-field calculations and renormalization-group treatments predict qualitatively different behaviors: for the infinite-shear model, a tricritical point appears in the temperature-pressure phase diagram, under the mean-field approach, whereas renormalization-group calculations yield only first-order transitions.

The studies on the compressibility of ferromagnetic models have shown that the critical exponent α (for the specific heat) displays a peculiar behavior. If it is positive for the rigid model, the corresponding compressible model exhibits only first-order transitions. If it is negative, the compressible case displays only second-order transitions, with the same critical exponents of the rigid model.[17,20] Theoretical and experimental studies also reveal that the exponent α is generally positive for systems with scalar order parameter and negative for $n \geqslant 2$. Thus, the order of the Ising transition ($n=1$) is changed in the presence of spin-lattice coupling, while models like XY or Heisenberg still exhibit continuous transitions, in spite of the compressibility. The shearless ferromagnetic model represents a separate case, since the critical exponents for constant volume are Fisher renormalized,[34] with $\alpha_{Fisher}=-\alpha_{rigid}/(1-\alpha_{rigid})$, which makes α_{Fisher} negative, while constant pressure critical exponents remain Ising-like.

Metamagnetic Ising systems under pressure have also been studied previously under mean-field approaches.[22,24] The shearless model, in the spirit of Baker and Essam, presents a phase diagram which is essentially the same as that of the rigid model.[22] The tricritical temperature was explicitly determined as a function of pressure and a possible relation to experimental data[23] was proposed. A compressible metamagnetic model in a lattice with Domb-like infinite shear forces presents other possible topologies for the phase diagram.[24] Depending on the values of the spin-lattice coupling, compressibility, and pressure, a second first-order transition line, at high temperatures and low fields, appears together with the usual low temperature, high field coexistence line. In such cases, a continuous transition line joins smoothly the two first-order transition lines, one at low temperature and the other at high temperature, and two tricritical points appear in the phase diagram. For the usual rigidlike phase diagram, the qualitative evolution of the tricritical point as a function of pressure was compared to experimental data,[25] suggesting particular forms for the interaction constants of the different systems.

A treatment based on the renormalization-group ideas to the rigid metamagnetic model yields the same phase diagram type as predicted by the mean-field approach.[9] The critical exponents of the fixed point related to the metamagnetic transition are Ising-like, and those related to the tricritical point are classical (Gaussian). It has been noted that for models with $n=1$, the tricritical exponents are classical in $d=3$,

but the same does not occur for models where $n=2$.[9] Although the order parameter of the model corresponds to $n=2$, the renormalized Hamiltonian presents an Ising character.

There are, thus, two reasons to investigate the compressible metamagnetic model through a renormalization-group analysis: (i) the different behaviors predicted by mean field, depending on the strength of the shear forces, and (ii) the discrepancy in the results of mean-field and renormalization-group techniques, seen in the case of ferromagnets.

More recently, compressibility of both ferro- and antiferromagnetic Ising systems, introduced through lattice distortions, has been looked at quite thoroughly under Monte Carlo simulations. Phase behavior and criticality obtained from these studies are quite different from the mean-field or field-theory predictions. In the ferromagnetic case, the zero field transition is critical, as in the rigid case, but the critical exponents are mean field[26,27] if a constant pressure ensemble is used. Under the constraint of constant volume, a completely different picture emerges, and a closed first-order line is present in the field-temperature phase diagram, which encloses a peculiar ordered phase.[28] For antiferromagnets, the two ensembles yield an Ising critical line in the field-temperature phase diagram.[29,30] Thus, in the face of such conflicting results, the question of compressibility remains unanswered. An overview of the status of the Monte Carlo simulations on the Ising systems at constant pressure or constant volume can be appreciated in the recent review article by Landau.[31]

This paper is organized as follows: in the next section, the model Hamiltonian is defined and transformed to continuous spin variables. In Sec. III, we perform a mean-field transformation in momentum space. In Sec. IV, the Hamiltonian is expanded around the mean field variables. In Sec. V, we detail the renormalization-group (RG) transformations. Section VI is devoted to the analysis of the recursion relations. In Sec. VII, we list the fixed points. In Sec. VIII, we present the general flow diagrams for the reduced Hamiltonian. In Sec. IX, we analyze the phase diagram of the compressible metamagnet. Finally, in Sec. X, we present our main conclusions. There are also two appendixes: the first presents some ingredients of the mean-field treatment, and the second concerns the expansion of the Hamiltonian.

II. MODEL HAMILTONIAN

We consider a compressible metamagnetic model with the same elastic features of Domb's ferromagnetic model.[13] The elastic deformations are homogeneous and isotropic, implying infinite-shear forces. The magnetic interactions are considered linearly dependent on intermolecular distance. Magnetic moments are Ising spin variables on a hypercubic lattice, in d space dimensions, divided into two interpenetrating sublattices. The sublattices are the alternating layers of $(d-1)$ dimensions of the lattice. The exchange interaction between first neighboring spins on the same sublattice is of the ferromagnetic type, while the coupling between neighboring spins belonging to different sublattices is of the antiferromagnetic type. The Hamiltonian of the model is given by

$$\mathcal{H} = -\frac{1}{2}\sum_{\langle ij\rangle} \sigma_i[J_{ij} - j_{ij}(a-a_0)]\sigma_j + \frac{1}{4}\sum_{\langle ij\rangle} K(a-a_0)^2 - \sum_i H_i\sigma_i, \tag{1}$$

where $\sigma_i = \pm 1$ are the spin variables and a_0 is the average distance between neighboring spins at a reference temperature and pressure. The elastic energy of the lattice is represented by the harmonic potential between nearest neighbor pairs of spins, where K is the elastic constant and a is the average distance between neighboring spins at temperature T. The linear approximation for the dependence of the magnetic coupling $J_{ij}(a)$ on the lattice constant a is justified by the large magnitude of K, so that only a small deformation is permitted for a fixed value of the external pressure. In this approximation, where we assume that the volume changes linearly with the deformation, the integral over volume becomes a simple Gaussian integration. Within the hyperplanes the interaction is ferromagnetic, $J_{ij} \equiv J_F$ and $j_{ij} \equiv j_F$, while between them it is antiferromagnetic, $J_{ij} \equiv -J_A$ and $j_{ij} \equiv -j_A$. H_i is the magnetic field at site i, which we take in the direction **1** of the anisotropy axis, perpendicular to the hyperplanes.

In order to introduce pressure (p) into the problem, we make a Laplace transformation from the canonical to the pressure ensemble, integrating over the elastic degrees of freedom. A biquadratic term appears and a Gaussian transformation is performed to linearize the functional. As a result of these transformations, a new variable y is introduced (see details in Ref. 24). The new free-energy functional Φ becomes

$$\Phi(y,[\sigma_i],T,p,[H_i]) = -\frac{y^2}{2} + \frac{1}{2}\sum_{ij} \sigma_i L_{ij}\sigma_j + \beta\sum_i H_i\sigma_i, \tag{2}$$

where $[\sigma_i]$ and $[H_i]$ mean the set of all spin and magnetic field variables of the system, respectively, and $\beta = 1/k_BT$ is the inverse temperature, with k_B being Boltzmann's constant. The coupling matrix,

$$L_{ij} = \beta\left(J_{ij} + \frac{pa_0^{d-1}}{K} j_{ij}\right) + y\sqrt{\frac{\beta}{dNK}}\, j_{ij}, \tag{3}$$

depends mainly on the exchange constant J_{ij}, but if the pressure differs from its reference value, $p=0$, the interaction changes in accordance with the spin-lattice coupling, j_{ij}.

In order to sum over spin variables, we perform a Hubbard-Stratonovich transformation, which introduces continuous variables as usual in the RG technique.[32] This yields

$$\Phi(y,[x_i],T,p,[H_i]) = -\frac{y^2}{2} - \frac{1}{2}\sum_{i,j} x_i L_{ij}^{-1} x_j + \sum_i \ln[2\cosh(x_i + \beta H_i)], \tag{4}$$

written in terms of x_i, which will play the role of spin variables. The last term on the right-hand side of the above equation comes from the summation over the old σ_i variables.

The inverse matrix for the couplings L_{ij}^{-1} [Eq. (3)] is diagonal in momentum space. Because the matrix elements L_{ij} depend only on the relative positions of the sites, $\mathbf{\Delta}_{ij}=\mathbf{r}_j-\mathbf{r}_i$, the Fourier transform of L_{ij} is written as

$$\tilde{L}(\mathbf{q})=\sum_{\mathbf{\Delta}_{ij}} L_{ij}\exp(-i\mathbf{q}\cdot\mathbf{\Delta}_{ij}). \tag{5}$$

The components of vetor $\mathbf{q}$ in the ν direction are given by $q_\nu=2\pi n_\nu/n$, with $0\leqslant n_\nu\leqslant n$, where $n^d=N$. Thus, we get

$$\tilde{L}(\mathbf{q})=2L_F\sum_{\nu=2}^{d}\cos q_\nu-2L_A\cos q_1. \tag{6}$$

Since $\tilde{L}(\mathbf{q})$ is diagonal, $\tilde{L}^\omega(\mathbf{q})=[\tilde{L}(\mathbf{q})]^\omega$, where ω is a real number. So, we can write

$$L_{ij}^\omega=\frac{1}{N}\sum_{\mathbf{q}}[\tilde{L}(\mathbf{q})]^\omega\exp(i\mathbf{q}\cdot\mathbf{\Delta}_{ij}). \tag{7}$$

III. MEAN-FIELD APPROXIMATION

The RG technique includes fluctuation effects into the Landau picture. We, thus, need to obtain the mean-field solution around which the free-energy functional must be expanded. Our approach is to adopt a Curie-Weiss Hamiltonian in which the interactions L_{ij} are rescaled and turned long range, which implies a new coupling matrix $\tilde{L}_{MF}(\mathbf{q})$ in momentum space. The original lattice can be thought of as a stack of ferromagnetic hyperplanes A and B, with an antiferromagnetic coupling between them. Fourier transformation of the mean-field long-range couplings will require partial sums over A and B hyperplanes, where the sum of a geometric series will be used, $\Sigma_{i=0}^{l-1}b^i=(1-b^l)/(1-b)$. In the direction $\mathbf{1}$, the A hyperplanes are located at $r_1^A=2j$ and the B hyperplanes at $r_1^B=2j+1$, where $j=0,1,\ldots,\frac{n}{2}-1$. Partial sums like $\Sigma_{r_1^{A,B}}\exp(iq_1r_1)$ over A or B vanish, except for $n_1=0$ and $n_1=n/2$. Thus, we get

$$\sum_{\mathbf{r}_{A,B}}\exp(i\mathbf{q}\cdot\mathbf{r})=\frac{N}{2}[\delta(\mathbf{q})\pm\delta(\mathbf{q}-\pi\mathbf{1})], \tag{8}$$

where the sign + (−) refers to A (B) and δ is Dirac's delta function. Finally, used in Eq. (5), this leads to

$$\tilde{L}_{MF}(\mathbf{q})=[(d-1)L_F-L_A]\delta(\mathbf{q})+[(d-1)L_F-L_A]\delta(\mathbf{q}-\pi\mathbf{1}). \tag{9}$$

Comparison of Eqs. (6) and (9) allow us to write the useful relation

$$\tilde{L}_{MF}(\mathbf{q})=[\tilde{L}(\mathbf{q})][\delta(\mathbf{q})+\delta(\mathbf{q}-\pi\mathbf{1})]. \tag{10}$$

After Fourier transformation of the spinlike continuous variables, with

$$x_i=\frac{1}{N}\sum_{\mathbf{q}}\tilde{x}(\mathbf{q})\exp(i\mathbf{q}\cdot\mathbf{r}_i), \tag{11}$$

minimization of the free-energy functional (4) in momentum space, under this approximation for the coupling matrix, automatically yields uniform solutions. The total magnetization m is related to $\tilde{x}(0)=\Sigma_i x_i$ and the order parameter, the staggered magnetization m_s, to $\tilde{x}(\pi\mathbf{1})=\Sigma_{i\in A}x_i-\Sigma_{i\in B}x_i$. The full mean-field solutions are given in Appendix A.

IV. EXPANSION OF THE HAMILTONIAN

To expand $\Phi(y,[x_i],T,p,[H_i])$ around the mean-field solution $\bar{\Phi}$, we define $y=\bar{y}+\Delta y$ and $x_i=\overline{x_i}+s_i$, where Δy and s_i represent small fluctuations. The expansion in Δy is taken up to second order due to the sharp maximum of Φ at $\bar{y}$. For the s_i variables, as usual, we keep terms up to fourth order to investigate the critical behavior.[33] The linear terms are eliminated due to Eqs. (A3) and (A4). The expanded Hamiltonian in the real space is shown in Appendix B 1

Firstly, we integrate over Δy. Defining the Fourier series for the fluctuations, $s_i=\frac{1}{N}\Sigma_{\mathbf{q}}\tilde{s}(\mathbf{q})\exp(i\mathbf{q}\cdot\mathbf{r}_i)$, and using Eqs. (7) and (A2)–(A6) into the functional (B1), we get

$$\begin{aligned}\Phi=\bar{\Phi}&-\sum_{\mathbf{q}}\phi_2^+\tilde{s}_q^+\tilde{s}_{-q}^+-\sum_{\mathbf{q}}\phi_2^\pm\tilde{s}_q^+\tilde{s}_{-q}^--\sum_{\mathbf{qq}'}\phi_3^+\tilde{s}_q^+\tilde{s}_{q'}^+\tilde{s}_{-q-q'}^+\\&-\sum_{\mathbf{qq}'}\phi_3^\pm\tilde{s}_q^+\tilde{s}_{q'}^+\tilde{s}_{-q-q'}^-+\left(\mu_0^+\tilde{s}_0^++\mu_0^-\tilde{s}_0^-+\sum_{\mathbf{q}}\mu_q^+\tilde{s}_q^+\tilde{s}_{-q}^+\right)^2\\&-\sum_{\mathbf{q},\mathbf{q}',\mathbf{q}''}\phi_4^+\tilde{s}_q^+\tilde{s}_{q'}^+\tilde{s}_{q''}^+\tilde{s}_{-q-q'-q''}^+-\sum_{\mathbf{q},\mathbf{q}',\mathbf{q}''}\phi_4^\pm\tilde{s}_q^+\tilde{s}_{q'}^+\tilde{s}_{q''}^+\tilde{s}_{-q-q'-q''}^-.\end{aligned} \tag{12}$$

The coefficients are given in Appendix B 2. We used the compact notation:

$$\tilde{s}_q^+=\tilde{s}(\mathbf{q}),\quad \tilde{s}_q^-=\tilde{s}(\mathbf{q}+\pi\mathbf{1}),\quad \tilde{s}_0^\pm=\tilde{s}_{q=0}^\pm. \tag{13}$$

The dependence of $\bar{\Phi}$ on $\tilde{s}_q$ is of the form $\tilde{s}_q^p/N^{p-1}$, implying that large powers of N must vanish in the thermodynamic limit.

We are going to define the order parameter of the model. In working with the functional (B1), any magnetic order must be associated with $\tilde{x}(\mathbf{q})$. However, we have defined the fluctuations s_i around the mean-field behavior. Then, $\tilde{s}_q^+$ is a measure of the coherence of the fluctuations and $\tilde{s}_q^-$ is the metamagnetic order parameter in the fluctuation space.

Different contributions appear due to the compressibility, to say, $\tilde{s}_0^+$ and $\tilde{s}_0^-$, respectively, the sum and the difference of the total fluctuations of the sublattices. They originate from the integration of the elastic degrees of freedom, and the last one will disappear from the Hamiltonian, but $\tilde{s}_0^+$ is a fundamental variable of the model. In the work of Bruno and Sak[17] about the renormalization group for the first-order transition of a compressible Ising magnet, $\tilde{s}_0^+$ is also present. These abnormal contributions are associated with the intrinsic mean-field character of the model, which arise from the prevention of elastic fluctuations in the system. They do not appear in the ferromagnetic case (Domb) because the magnetization is zero, vanishing contribution μ_0^+ in Eq. (12).

We have expanded the spin variables around the mean-field ones, but these variables are only defined for $\mathbf{q}=\mathbf{0}$ and $\mathbf{q}=\pi\mathbf{1}$. However, the momentum q in the functional (12) is any number in the interval $[0,2\pi]$. Thus, we must restrict $\mathbf{q}$

to be small around $\mathbf{q}=\mathbf{0}$ and $\mathbf{q}=\pi\mathbf{1}$, but first, we rewrite Eq. (12) by breaking the sums into two parts, beginning, respectively, at $\mathbf{q}=\mathbf{0}$ and $\mathbf{q}=\pi\mathbf{1}$. Nelson and Fisher, in their work about RG of the rigid metamagnetic model,[9] implemented a different scheme to retain the distinction of the spin variables. We use a simple transformation, valid for all periodic function of period 2π, which naturally reveals all the occurrences of $\tilde{s}_q^-$,

$$\sum_{\theta=0}^{2\pi} f(\theta) = \sum_{\theta=0}^{2\pi} f(\theta+\pi) = \frac{1}{2}\sum_{\theta=0}^{2\pi}[f(\theta)+f(\theta+\pi)]. \quad (14)$$

Applying this recipe to Φ [Eq. (12)], we get contributions of the type

$$\sum_{\mathbf{q},\mathbf{q}'} \tilde{s}_q^+\tilde{s}_{q'}^+\tilde{s}_{-q-q'}^+ = \frac{1}{4}\sum_{\mathbf{q},\mathbf{q}'}(\tilde{s}_q^+\tilde{s}_{q'}^+\tilde{s}_{-q-q'}^+ + 3\tilde{s}_q^+\tilde{s}_{q'}^-\tilde{s}_{-q-q'}^-). \quad (15)$$

Near the phase transition, the correlation length is large, and only small values of q need to be considered. To obtain the appropriate form of the Hamiltonian, we must expand $L^{-1}(\mathbf{q})$ in the ϕ_2 coefficients of Eq. (12) around $q=0$ up to second order. It is not necessary to consider other powers of q, because they are irrelevant for all fixed points.[17,33] The sums in $\mathbf{q}$ are transformed into integrals, $\frac{1}{N}\Sigma_{\mathbf{q}} \to \frac{1}{\Omega}\int d\mathbf{q} \equiv \int_{\mathbf{q}}$, where $\Omega=(2\pi)^d$ is the volume of integration. Henceforth, this compact notation will be used.

In the vicinity of the critical point, the system is disordered and we can put $m_s=0$. Finally, as usual, we make a transformation to write the coefficient of $\mathbf{q}$ in the $\tilde{s}_q^-\tilde{s}_{-q}^-$ term equal to the unit $q_\nu=c_1 q'_\nu$, for $\nu=2,3,\ldots,d$ and $\tilde{s}_q^-=c_2 s_q^-$, where $c_1=(L_A/L_F)^{1/2}$ and $c_2=[c_1^{d-1}L_A/L^2(\pi\mathbf{1})]^{-1/2}$. After these transformations, we have

$$\begin{aligned}\Phi = \bar{\Phi} &- \frac{1}{2}\int_{\mathbf{q}}\left[r(\mathbf{0})+e\left(\sum_{\nu=2}^{d} q_\nu^2 - q_1^2\right)\right]s_q^+ s_{-q}^+ \\ &- \frac{1}{2}\int_{\mathbf{q}}[r(\pi\mathbf{1})+\mathbf{q}^2]s_q^- s_{-q}^- + \frac{1}{2\Omega\kappa}\left[c_2\frac{Q(\mathbf{0})}{L(\mathbf{0})}ms_0^+\right. \\ &\left. + \frac{1}{4}\int_{\mathbf{q}}\frac{eQ(\mathbf{0})}{L_A}s_q^+ s_{-q}^+ + \frac{1}{4}\int_{\mathbf{q}}\frac{Q(\pi\mathbf{1})}{L_A}s_q^- s_{-q}^-\right]^2 \\ &- w\int_{\mathbf{q}}\int_{\mathbf{q}'}(s_q^+ s_{q'}^+ s_{-q-q'}^+ + 3s_q^+ s_{q'}^- s_{-q-q'}^-) \\ &- u\int_{\mathbf{q}}\int_{\mathbf{q}'}\int_{\mathbf{q}''}(s_q^+ s_{q'}^+ s_{q''}^+ s_{-q-q'-q''}^+ + 6s_q^+ s_{q'}^+ s_{q''}^- s_{-q-q'-q''}^- \\ &+ s_q^- s_{q'}^- s_{q''}^- s_{-q-q'-q''}^-). \end{aligned} \quad (16)$$

Additional parameters are defined in Appendix B 3.

As previously commented, a treatment of the first-order transition of Domb's model with renormalization group[17] reveals spontaneous appearance of s_0^+. If in the functional (16) we put $s_q^-=0$, it is reduced to that cited work. Below the first-order transition temperature, the system is ordered and, supposing large correlation length of the spin variables, the RG can be applied. In that work are calculated the free energy, susceptibility, equation of state, etc.

In the absence of fluctuations, a mean-field analysis would show that $r(\pi\mathbf{1})=0$ and $r(\mathbf{0})>r(\pi\mathbf{1})$.[24,35] Due to the nearness of the mean-field solution, this is the actual situation in the starting functional (16). The rescale of the RG transformation will be defined as a function of the quadratic terms, and this fact will be of fundamental importance in the selection of the fields to be fixed.

V. RENORMALIZATION-GROUP TRANSFORMATIONS

To generate the RG recursion relation, we assume, as usual, that the nonquadratic parts of the Hamiltonian are small and can be calculated by perturbation theory.[33] A new renormalized Hamiltonian is generated from Φ by integrating out the spin variables $s_q^\pm$ of momentum $\Lambda/b<q<\Lambda$. We have considered a spherical Brillouin zone of radius Λ and a rescaling factor $b>1$. The Hamiltonian is restored to its original form by a rescaling factor b for the momentum and by factors ζ for the spin variables.

Now, we consider that the RG transformation is carried out many times and the coefficients are changed. The integrations left out only small domains around $\mathbf{q}=\mathbf{0}$ and $\mathbf{q}=\pi\mathbf{1}$. Rescaling recovers the integration limits, $0<q<\Lambda$, and the modified Hamiltonian takes the general form

$$\begin{aligned}\Phi_r = &-\frac{1}{2}\int_{\mathbf{q}\neq 0}\left[r_+ + e_+\left(\sum_{\nu=2}^{d} q_\nu^2 - q_1^2\right)\right]s_q^+ s_{-q}^+ \\ &- \frac{1}{2}\int_{\mathbf{q}}[r_- + e_-\mathbf{q}^2]s_q^- s_{-q}^- - w_+\int_{\mathbf{q}\neq 0}\int_{\mathbf{q}'\neq 0} s_q^+ s_{q'}^+ s_{-q-q'}^+ \\ &- w_-\int_{\mathbf{q}\neq 0}\int_{\mathbf{q}'} s_q^+ s_{q'}^- s_{-q-q'}^- + \frac{B_+}{\Omega}\left(\int_{\mathbf{q}\neq 0} s_q^+ s_{-q}^+\right)^2 \\ &+ \frac{B_\pm}{\Omega}\left(\int_{\mathbf{q}\neq 0} s_q^+ s_{-q}^+\right)\left(\int_{\mathbf{q}'} s_{q'}^- s_{-q'}^-\right) \\ &+ \frac{B_-}{\Omega}\left(\int_{\mathbf{q}} s_q^- s_{-q}^-\right)^2 - \Phi_{4r} + \Phi_{0r}, \end{aligned} \quad (17)$$

where

$$\begin{aligned}\Phi_{4r} = &\, u_+\int_{\mathbf{q}\neq 0}\int_{\mathbf{q}'\neq 0}\int_{\mathbf{q}''\neq 0} s_q^+ s_{q'}^+ s_{q''}^+ s_{-q-q'-q''}^+ \\ &+ u_\pm\int_{\mathbf{q}\neq 0}\int_{\mathbf{q}'\neq 0}\int_{\mathbf{q}''} s_q^+ s_{q'}^+ s_{q''}^- s_{-q-q'-q''}^- \\ &+ u_-\int_{\mathbf{q}}\int_{\mathbf{q}'}\int_{\mathbf{q}''} s_q^- s_{q'}^- s_{q''}^- s_{-q-q'-q''}^-, \end{aligned} \quad (18)$$

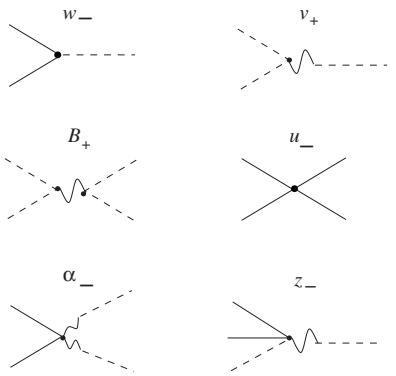

FIG. 1. Some primitive Feynman diagrams which take part of the Hamiltonian. The respective coefficients are indicated above the graphs. The point is the ordinary vertex and the tilde is the vertex coming from the compressibility contribution and does not carry any momentum. Solid lines denote the propagator G_-, dashed lines the G_+.

$$\Phi_{0r} = -\frac{1}{2\Omega} r_0 s_0^{+2} - \frac{v_+}{\Omega} s_0^+ \int_{\mathbf{q}\neq 0} s_q^+ s_{-q}^+ - \frac{v_-}{\Omega} s_0^+ \int_{\mathbf{q}} s_q^- s_{-q}^- - \frac{v_0}{\Omega^2} s_0^{+3}$$
$$+ \frac{\alpha_+}{\Omega}\frac{s_0^{+2}}{\Omega} \int_{\mathbf{q}\neq 0} s_q^+ s_{-q}^+ + \frac{\alpha_-}{\Omega}\frac{s_0^{+2}}{\Omega} \int_{\mathbf{q}} s_q^- s_{-q}^- + \frac{\alpha_0}{\Omega^3} s_0^{+4}$$
$$- z_+ \frac{s_0^+}{\Omega} \int_{\mathbf{q}\neq 0} \int_{\mathbf{q}'\neq 0} s_q^+ s_{q'}^+ s_{-q-q'}^+$$
$$- z_- \frac{s_0^+}{\Omega} \int_{\mathbf{q}\neq 0} \int_{\mathbf{q}'} s_q^+ s_{q'}^- s_{-q-q'}^-, \tag{19}$$

and $e_-=1$ remains fixed.

The terms containing the variable s_0^+ were written separately in Φ_{0r}, in order to distinguish them from the ordinary contribution s_q^+ with $q\neq 0$. The coefficients of fourth-order terms in Φ_{0r} are linear combinations of the respective coefficients of Φ_r, but the others have independent contributions. They lead to a different class of contribution in the renormalization process, and this separation is convenient by technical reasons. The new coefficients v can have any sign, but B_+ and B_- are always positive.

The perturbation theory involves two distinct Feynman propagators associated with the variables s_q^+ and s_q^-, respectively,

$$G_+(\mathbf{q}) = \left[r_+ + e_+ \left(\sum_{\nu=2}^{d} q_\nu^2 - q_1^2 \right) \right]^{-1}, \quad G_-(\mathbf{q}) = [r_- + e_- \mathbf{q}^2]^{-1}. \tag{20}$$

The Feynman graphs that appear in this problem include two types of legs and vertices. Figure 1 shows the primitive Feynman diagrams that appear in the Hamiltonian. The dashed lines represent s_q^+ and the continuous lines represent s_q^-. The ordinary vertex is represented by a dot and the vertex coming from the compressibility contribution by a tilde. It does not carry any momentum. All dashed lines that appear alone at the end of a tilde represent s_0^+.

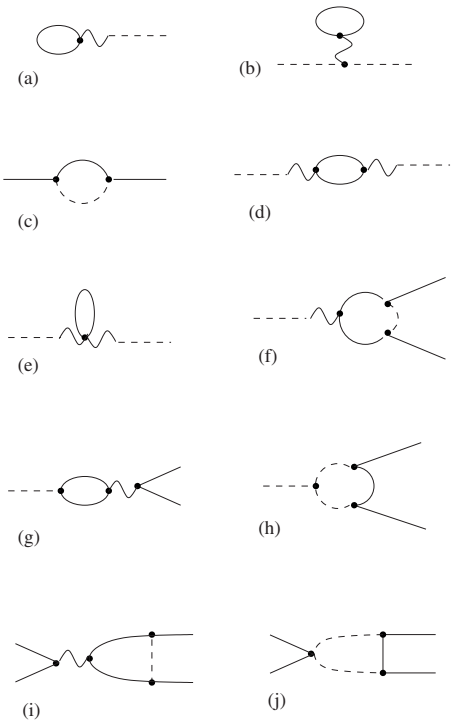

FIG. 2. Some graphs involved in the calculations of the recursion relations. The respective equations are (a) Eq. (31), (b) Eq. (23), (c) Eq. (24), (d) Eq. (26), (e) Eq. (26), (f) Eq. (27), (g) Eq. (27), (h) Eq. (28), (i) Eq. (29), and (j) Eq. (30).

By defining the rescaling factors in $\mathbf{q}$ and $s_q^\pm$, we are able to write the recursion equations. The limits of integration are restored by doing $|\mathbf{q}'|=b|\mathbf{q}|$. For the rigid metamagnetic model, there are two classes of spin variables and two rescaling factors, but for the compressible version of the model, due to the specific contributions of the coefficients r_0 and $v_\pm$, we must use three scaling factors,

$$s_q^+ = \zeta_+ s_{q'}^{+\prime}, \quad s_q^- = \zeta_- s_{q'}^{-\prime}, \quad s_0 = \zeta_0 s_0^{+\prime}. \tag{21}$$

VI. RECURSION RELATIONS

In this work, we consider perturbation theory to first order in ϵ, where $\epsilon=4-d$. It is well known[33] that for the Ising model, the only nonzero coefficients in Eq. (17) are r_-, e_-, and u_-, and that the fixed points are $u_-=O(\epsilon)$ and $r_-=O(\epsilon)$. In the case of the rigid metamagnetic model,[9] an additional field is required, w_-, proportional to the magnetic field. It becomes important when $w_-=O(\epsilon^{1/2})$. The compressible ferromagnetic models correspond to $w_-=0$ and $B_-\neq 0$, and presents a new fixed point $B_-=O(\epsilon)$.[17] Let us consider the relevant contributions, for which all the quadratic terms have fixed points of $O(\epsilon)$, all the third-order terms of $O(\epsilon^{1/2})$, and all the fourth-order terms of $O(\epsilon)$.

Some of the Feynman graphs involved in the calculation of the recursion relations are presented in Fig. 2. Consider the integral

$$I_{kl} = \int_{\mathbf{p}} [G_+(p)]^k [G_-(p)]^l, \tag{22}$$

where $\Lambda \geqslant p > \Lambda/b$. The integral related to graphs (a) and (b) of Fig. 2 is represented by I_{01} [it is equal to $(b^2-1)/16b^2$ for $\Lambda=\pi$]. It can be shown[9,35] that the integral represented by graphs (d) and (g) of Fig. 2 is weakly dependent on $\mathbf{q}$. We will not consider this dependence and we denote that integral by I_{02} $(=\ln b/8\pi_2)$. All integrals which appear in the recursion equations can be reduced to I_{02}. This fact helps us, allowing us to write the Feynman integrals without differences on $\mathbf{q}$ dependences.

To simplify the presentation, we list below only the recursion relations for the relevant variables. To the leading order in ϵ, they are

$$\overline{r_+} = \zeta_+^2 b^{-d}[r_+ - 4B_+I_{10} - 2B_\pm I_{01} + 12u_+I_{10} + 2u_\pm I_{01} - 18w_+^2 I_{20} - 2w_-^2 I_{02} + O(\epsilon^2)], \tag{23}$$

$$\overline{r_-} = \zeta_-^2 b^{-d}[r_- - 4B_-I_{01} - 2B_\pm I_{10} + 12u_-I_{01} + 2u_\pm I_{10} - w_-^2 I_{11} + O(\epsilon^2)], \tag{24}$$

$$\overline{e_\pm} = \zeta_\pm^2 b^{-d-2}[e_\pm + O(\epsilon^2)], \tag{25}$$

$$\overline{r_0} = \zeta_0^2 b^{-d}[r_0 - 2v_+^2 I_{20} - 2v_-^2 I_{02} - 2\alpha_+ I_{10} - 2\alpha_\pm I_{01} + O(\epsilon^2)], \tag{26}$$

$$\overline{v_-} = \zeta_0\zeta_-^2 b^{-2d}[v_- + 2v_+B_\pm I_{20} + 4v_-B_-I_{02} + 4v_-w_-^2 I_{12} + 4v_+w_-^2 I_{21} - 2v_-u_-I_{02} - 2v_+u_\pm I_{20} + 4w_-z_-I_{11} + O(\epsilon^{5/2})], \tag{27}$$

$$\overline{w_-} = \zeta_+\zeta_-^2 b^{-2d}[w_- - 12w_-u_-I_{02} - 6w_+u_\pm I_{20} - 8w_-u_\pm I_{11} + 12w_+w_-^2 I_{21} + 4w_-^3 I_{12} + O(\epsilon^{5/2})], \tag{28}$$

$$\overline{B_-} = \zeta_-^4 b^{-3d}[B_- + 4B_-^2 I_{02} + B_\pm^2 I_{20} - 24B_-u_-I_{02} - 2B_\pm u_\pm I_{20} + 4B_\pm w_-^2 I_{21} + 8B_-w_-^2 I_{12} + O(\epsilon^3)], \tag{29}$$

$$\overline{u_-} = \zeta_-^4 b^{-3d}[u_- - 36u_-^2 I_{02} - u_\pm^2 I_{20} + 24u_-w_-^2 I_{12} + 4u_\pm w_-^2 I_{21} - 4w_-^4 I_{22} + O(\epsilon^3)]. \tag{30}$$

Two remarks must be made. If we had carried out these transformations in real space, each RG transformation would divide the lattice into blocks of spins of side b.[33] To this new lattice, we ought to associate an exchange constant b times larger than the original one and a volume b^d times smaller, in units of the new lattice constant. As the terms related to the spin-lattice coupling carry the volume Ω (in the momentum space), the rescaling of $\mathbf{q}$ would produce a b^{-d} factor in the recursion relations $(\Omega=b^d\Omega')$. The second point concerns the order of correction of $\bar{e}$, which comes from the fact that the integrals which occur in the recursion relations of the quadratic terms have no dependence on $\mathbf{q}$, as explained previously.

Besides these equations, a linear term is also generated [see Fig. 2(a)], whose coefficient is

$$-\zeta_0[v_+I_{10} + v_-I_{01} + O(\epsilon^{3/2})]. \tag{31}$$

The three leg graphs give rise to these fields, which are proportional to the magnetic field, both for the compressible and rigid cases.[9] It causes an instability, turning aside the RG transformation from criticality. We can fix this problem by a secondary shift of variables,

$$s_0^+ = s_0^{+\prime} + \Omega M, \tag{32}$$

and choosing M to cancel the linear terms. The transformation will generate new terms of first, second, and third order in the Hamiltonian Φ_r [Eq. (17)].

It is usual to choose ζ to keep constant the coefficients of $\mathbf{q}^2$ (in this case, e_+ and e_-). Looking at Eqs. (23) and (24), we see that r_+ and r_- scale as b^2, but as $r_+ > r_-$ in the initial Hamiltonian, r_+ must diverge when r_- is at criticality. Consequently, the propagator $G_+(\mathbf{q})$ approaches zero, meaning that one loses control over the s_q^+ variables. To avoid this, we perform a rescaling in order to keep r_+ fixed in place of e_+, while keeping $e_-=1$, as usual. The factor ζ_0 is naturally chosen to keep fixed r_0.

To reduce the number of variables, we shall first obtain the rescaling constant ζ to order ϵ^0, and verify which fields are irrelevant, in order to discard them. Applying the secondary transformation [Eq. (32)] to Φ_r [Eq. (17)], we get

$$r_+' = \overline{r_+} + 2\overline{v_+}M - 2\overline{\alpha_+}M^2,$$

$$r_0' = \overline{r_0} + 6\overline{v_0}M + 12\overline{\alpha_0}M^2, \quad e_-' = \overline{e_-}. \tag{33}$$

We shall see below that M is of order $\epsilon^{1/2}$, and to obtain ζ to order ϵ^0, the above correction will be temporarily discarded. Using Eqs. (23), (25), and (26), we obtain $\zeta_+=b^{2-(\epsilon/2)}[1+O(\epsilon)]$, $\zeta_-=b^{3-(\epsilon/2)}[1+O(\epsilon^2)]$, and $\zeta_0=b^{2-(\epsilon/2)}[1+O(\epsilon)]$.

Now it is easy to verify which fields are irrelevant. For example, $w_+'=b^{-2+(\epsilon/2)}[w_+ + O(\epsilon^{3/2})]$ is strongly irrelevant and vanishes through the RG transformations. In the same way, e_+, v_0, v_+, B_+, $B_\pm$, u_+, $u_\pm$, α_+, α_-, z_+, z_-, and α_0, are also all irrelevant. Other possible dependences on q which could occur in the Hamiltonian (e.g., in the biquadratic term) would be irrelevant for the same reason. Because of the irrelevance of the e_+ term, the integrals [Eq. (22)] take the simple form $I_{kl}=I_{0l}/r_+^k$.

Let us correct the rescaling factors ζ_+ and ζ_0 to order ϵ. Because v_+, α_+, v_0, and α_0 are irrelevant, we have $r_+'=\overline{r_+}$ and $r_0'=\overline{r_0}$ [see Eqs. (33), (23), and (26)], and

$$\zeta_+ = b^{2-(\epsilon/2)}\left[1 + I_{02}\frac{w_-^2}{r_+} + O(\epsilon^2)\right],$$

$$\zeta_0 = b^{2-(\epsilon/2)}\left[1 + I_{02}\frac{v_-^2}{r_0} + O(\epsilon^2)\right]. \tag{34}$$

The secondary shift of variables [Eq. (32)] produces nonzero contributions only to variables r_0 and v_-. Requiring the linear terms to vanish [Eq. (31)] from Eqs. (26) and (27), we obtain

$$M = -b^{2-(\epsilon/2)}\left[I_{01}\frac{v_-}{r_0} + O(\epsilon^{3/2})\right]. \tag{35}$$

TABLE I. Fixed points as functions of $\bar{\epsilon}=8\pi^2\epsilon$ and $c\bar{\epsilon}=\pi^2/2\epsilon$, and corresponding universality classes. G stands for Gaussian, I for Ising, GR for renormalized Gaussian (Ref. 34, $\nu=\frac{1}{2}+\frac{\epsilon}{4}$), and IR for renormalized Ising (Ref. 17).

*	u^*	W^*	B_-^*	V^*	r_-^*	
G_0	0	0	0	0	0	G
G_V	0	0	0	$-\bar{\epsilon}/2$	$-c\bar{\epsilon}$	GR
G_B	0	0	$-\bar{\epsilon}/4$	0	$-c\bar{\epsilon}$	GR
G_{VB}	0	0	$-\bar{\epsilon}/4$	$\bar{\epsilon}/2$	0	G
I_0	$\bar{\epsilon}/36$	0	0	0	$-c\bar{\epsilon}/3$	I
I_V	$\bar{\epsilon}/36$	0	0	$-\bar{\epsilon}/6$	$-2c\bar{\epsilon}/3$	IR
I_B	$\bar{\epsilon}/36$	0	$-\bar{\epsilon}/12$	0	$-2c\bar{\epsilon}/3$	IR
I_{VB}	$\bar{\epsilon}/36$	0	$-\bar{\epsilon}/12$	$\bar{\epsilon}/6$	$-c\bar{\epsilon}/3$	I
M_0	$\bar{\epsilon}/9$	$\bar{\epsilon}/6$	0	0	$-2c\bar{\epsilon}/3$	IR
M_V	$\bar{\epsilon}/9$	$\bar{\epsilon}/6$	0	$\bar{\epsilon}/6$	$-c\bar{\epsilon}/3$	I
M_B	$\bar{\epsilon}/9$	$\bar{\epsilon}/6$	$\bar{\epsilon}/12$	0	$-c\bar{\epsilon}/3$	I
M_{VB}	$\bar{\epsilon}/9$	$\bar{\epsilon}/6$	$\bar{\epsilon}/12$	$-\bar{\epsilon}/6$	$-2c\bar{\epsilon}/3$	IR
T_0	$\bar{\epsilon}/4$	$\bar{\epsilon}/2$	0	0	$-c\bar{\epsilon}$	GR
T_V	$\bar{\epsilon}/4$	$\bar{\epsilon}/2$	0	$\bar{\epsilon}/2$	0	G
T_B	$\bar{\epsilon}/4$	$\bar{\epsilon}/2$	$\bar{\epsilon}/4$	0	0	G
T_{VB}	$\bar{\epsilon}/4$	$\bar{\epsilon}/2$	$\bar{\epsilon}/4$	$-\bar{\epsilon}/2$	$-c\bar{\epsilon}$	GR

VII. FIXED POINTS

To make the analysis of the recursion relations easier, we define

$$W=\frac{w_-^2}{r_+},\quad V=\frac{v_-^2}{r_0},\tag{36}$$

which are always positive quantitites. After correcting the equation for v_- [Eq. (27)] due to the secondary shift of variables [Eq. (32)], we get the recursion relations in final form from Eqs. (27), (28), and (34)–(36). To leading order in ϵ, the set of equations (24)–(30) becomes

$$\delta r_- = r_-' - r_- = (b^2-1)r_- - b^2 I_{01}(4B_- - 12u_- + 4W + 2V),$$

$$\delta V = V' - V = V(\epsilon \ln b + 8I_{02}B_- - 24I_{02}u_- + 8I_{02}W + 2I_{02}V),$$

$$\delta W = W' - W = W(\epsilon \ln b - 24I_{02}u_- + 10I_{02}W),$$

$$\delta B_- = B_-' - B_- = B_-[\epsilon \ln b + 4I_{02}B_- - 24I_{02}u_- + 8I_{02}W],$$

$$\delta u_- = u_-' - u_- = u_-[\epsilon \ln b - 36I_{02}u_- + 24I_{02}W] - 4I_{02}W^2,\tag{37}$$

while $e_-=1$, and r_+ and r_0 remain fixed. Note that all the variables are of order ϵ. The respective fixed points are listed in Table I.

The fixed points are written in units of $\bar{\epsilon}=\frac{\epsilon \ln b}{I_{02}}=8\pi^2\epsilon$ and $c\bar{\epsilon}=\frac{b^2 I_{01}\ln b}{(b^2-1)I_{02}}\epsilon=\frac{1}{2}\pi^2\epsilon$ and are independent of b, as expected. The symbols for the fixed points are borrowed from the corresponding metamagnetic rigid model, for which $r_0=r_+$, $B_-=0$, and $V=W$ (see next section). For arbitrary (including nonphysical) values of the parameters of the compressible metamagnetic Hamiltonian, each of the fixed point of the rigid model decouples into four points.

A linearization of the recursion equations around the fixed points allows one to obtain the respective eigenvalues and eigenvectors. The linearized equations can be represented by $\boldsymbol{v}'=\Xi_b\boldsymbol{v}$, where $\boldsymbol{v}=[\varphi-\varphi^*]$ are vectors, φ are the variables of Eq. (37), and Ξ_b is the transformation matrix. The eigenvectors of Ξ_b are expressed in terms of four variables $\boldsymbol{v}_\lambda=(\delta u_-,\delta W,\delta B_-,\delta V)$. In Table II, we list the eigenvalues and eigenvectors related to the corresponding fixed points of Table I.

Critical exponents ν (correlation length) and η (two-point correlation function) indicate the universality classes of the fixed points.[33] The last column of Table I presents the universality class of each critical point (see Table II).

VIII. FLOW DIAGRAMS

Before examining the flow diagrams, we need to give a physical interpretation to the fields. Let us define new spin-lattice couplings

$$j_\pm=(d-1)j_F\pm j_A,\tag{38}$$

where j_F and j_A are the original spin-lattice coupling constants. Let us also assume null pressure, $p=0$. An inspection of the Hamiltonians given by Eqs. (16)–(19) shows that $B_-\sim[Q(\pi\mathbf{1})]^2\sim j_-^2/KJ_A^2$ [see Eq. (A1) in Appendix A], thus representing the compressibility term.[17] Moreover, the field W is proportional to the square of the magnetization, $W\sim m^2$ [see Eqs. (B4) in Appendix B], and therefore, to the square of the magnetic field (since $m\sim H$), as in the rigid model.[9] As to variable V, it is a sum of two fields, $V=W(1-\Sigma)$. $\Sigma\sim[Q(\mathbf{0})Q(\pi\mathbf{1})]\sim(j_-j_+)$ and shall be refered to as the anisotropy of the spin-lattice coupling. Note that the last result comes from (i) the contribution $\mathbf{q}=\mathbf{0}$ of the ordinary three leg term of coefficient w plus the corresponding contribution between square brackets in Eq. (16), and (ii) the contribution $\mathbf{q}=\mathbf{0}$ of the ordinary two leg term of coefficient r_+ plus the corresponding contribution between square brackets in Eq. (16). The new term $W\Sigma$ is proportional to the product of the squared magnetic field, H^2, with the anisotropy of the spin-lattice couplings (Σ). The alignment produced by the field is increased or decreased in accordance with the sign of the latter parameter.

We shall first discuss some particular cases.

The rigid metamagnetic model results from making $r_0=r_+$, $v_-=w_-$ ($V=W$), and $B_-=0$. For clarity, we adapt the flow diagram of Nelson and Fisher[9] to our notation in Fig. 3. The four fixed points (G_0, I_0, M_V, and T_V) and corresponding flow diagrams of the rigid model are shown in the $W\times u_-$ plane, which represents the cut $V=W$ in $(u_-,W,V,B=0)$ space. At zero magnetic field, the continuous phase transition is controlled by the fixed point I_0, which is Ising-like. If a magnetic field is applied, $W>0$, the trajectories run to the stable Ising-like fixed point M_V. Increasing W, and thus the magnetic field, the flows go to the Gaussian-like point T_V for $W=2u_-$. For higher fields, $W>2u_-$, the flows move away

TABLE II. Eigenvalues, eigenvectors, and critical exponents ν related to the fixed points of Table I. The correction of order ϵ in λ_r is due to $\frac{\partial I_{01}}{\partial r_-}=-I_{02}$.

*	G_0	G_V	G_B	G_{VB}
λ_1	ϵ	ϵ	ϵ	ϵ
v_1	(1, 0, 0, 0)	(1, 0, 0, 6)	(1, 0, 3, 0)	(1, 0, 3, 0)
λ_2	ϵ	ϵ	ϵ	ϵ
v_2	(0, 1, 0, 0)	(0,1,0,−2)	(0,1,−1,0)	(0,1,−1,0)
λ_B	ϵ	ϵ	$-\epsilon$	$-\epsilon$
v_B	(0, 0, 1, 0)	(0, 0, 1, 0)	(0, 0, 1, 0)	(0,0,1,−2)
λ_V	ϵ	$-\epsilon$	$-\epsilon$	ϵ
v_V	(0, 0, 0, 1)	(0, 0, 0, 1)	(0, 0, 0, 1)	(0, 0, 0, 1)
λ_r	2	$2-\epsilon$	$2-\epsilon$	2
ν	$\frac{1}{2}$	$\frac{1}{2}+\frac{\epsilon}{4}$	$\frac{1}{2}+\frac{\epsilon}{4}$	$\frac{1}{2}$
*	I_0	I_V	I_B	I_{VB}
λ_1	$-\epsilon$	$-\epsilon$	$-\epsilon$	$-\epsilon$
v_1	(1, 0, 0, 0)	(1,0,0,−6)	(1,0,−3,0)	(1,0,−3,0)
λ_2	$\frac{\epsilon}{3}$	$\frac{\epsilon}{3}$	$\frac{\epsilon}{3}$	$\frac{\epsilon}{3}$
v_2	(1, 2, 0, 0)	(1, 2, 0, 2)	(1, 2, 1, 0)	(1, 2, 1, 0)
λ_B	$\frac{\epsilon}{3}$	$\frac{\epsilon}{3}$	$-\frac{\epsilon}{3}$	$-\frac{\epsilon}{3}$
v_B	(0, 0, 1, 0)	(0,0,1,−2)	(0, 0, 1, 0)	(0,0,1,−2)
λ_V	$\frac{\epsilon}{3}$	$-\frac{\epsilon}{3}$	$-\frac{\epsilon}{3}$	$\frac{\epsilon}{3}$
v_V	(0, 0, 0, 1)	(0, 0, 0, 1)	(0, 0, 0, 1)	(0, 0, 0, 1)
λ_r	$2-\frac{\epsilon}{3}$	$2-\frac{2\epsilon}{3}$	$2-\frac{2\epsilon}{3}$	$2-\frac{\epsilon}{3}$
ν	$\frac{1}{2}+\frac{\epsilon}{12}$	$\frac{1}{2}+\frac{\epsilon}{6}$	$\frac{1}{2}+\frac{\epsilon}{6}$	$\frac{1}{2}+\frac{\epsilon}{12}$
*	M_0	M_V	M_B	M_{VB}
λ_1	$-\epsilon$	$-\epsilon$	$-\epsilon$	$-\epsilon$
v_1	(2, 3, 0, 0)	(2, 3, 0, 3)	$(2,3,\frac{3}{2},0)$	$(2,3,\frac{3}{2},-3)$
λ_2	$-\frac{\epsilon}{3}$	$-\frac{\epsilon}{3}$	$-\frac{\epsilon}{3}$	$-\frac{\epsilon}{3}$
v_2	(1, 2, 0, 0)	(1, 2, 0, 2)	(1, 2, 1, 0)	(1, 2, 1, 0)
λ_B	$-\frac{\epsilon}{3}$	$-\frac{\epsilon}{3}$	$\frac{\epsilon}{3}$	$\frac{\epsilon}{3}$
v_B	(0, 0, 1, 0)	(0,0,1,−2)	(0, 0, 1, 0)	(0,0,1,−2)
λ_V	$-\frac{\epsilon}{3}$	$\frac{\epsilon}{3}$	$\frac{\epsilon}{3}$	$-\frac{\epsilon}{3}$
v_V	(0, 0, 0, 1)	(0, 0, 0, 1)	(0, 0, 0, 1)	(0, 0, 0, 1)
λ_r	$2-\frac{2\epsilon}{3}$	$2-\frac{\epsilon}{3}$	$2-\frac{\epsilon}{3}$	$2-\frac{2\epsilon}{3}$
ν	$\frac{1}{2}+\frac{\epsilon}{6}$	$\frac{1}{2}+\frac{\epsilon}{12}$	$\frac{1}{2}+\frac{\epsilon}{12}$	$\frac{1}{2}+\frac{\epsilon}{6}$
*	T_0	T_V	T_B	T_{VB}
λ_1	ϵ	ϵ	ϵ	ϵ
v_1	(1, 3, 0, 0)	(1, 3, 0, 0)	(1, 3, 0, 0)	(1, 3, 0, 0)
λ_2	$-\epsilon$	$-\epsilon$	$-\epsilon$	$-\epsilon$
v_2	(1, 2, 0, 0)	(1, 2, 0, 2)	(1, 2, 1, 0)	(1, 2, 1, 0)
λ_B	$-\epsilon$	$-\epsilon$	ϵ	ϵ
v_B	(0, 0, 1, 0)	(0,0,1,−2)	(0, 0, 1, 0)	(0,0,1,−2)
λ_V	$-\epsilon$	ϵ	ϵ	$-\epsilon$
v_V	(0, 0, 0, 1)	(0, 0, 0, 1)	(0, 0, 0, 1)	(0, 0, 0, 1)
λ_r	$2-\epsilon$	2	2	$2-\epsilon$
ν	$\frac{1}{2}+\frac{\epsilon}{4}$	$\frac{1}{2}$	$\frac{1}{2}$	$\frac{1}{2}+\frac{\epsilon}{4}$

from the fixed points, indicating a discontinuous transition. Thus, T_V represents a tricritical point with Gaussian exponents.

The model with $r_+=r_0=V=W=0$ [see Eq. (17)] corresponds either to the ferromagnetic model of finite[16] or infinite shear[17,19] at fixed pressure (with $B_->0$) or to the Baker-Essam ferromagnetic model of zero shear at fixed volume (with $B_-<0$).[17,19] In the ferromagnetic case, there are four fixed points: G_0 (Gaussian), G_B (renormalized Gaussian), I_0 (Ising), and I_B (renormalized Ising).[14,17] The most stable fixed point is renormalized Ising I_B, which controls the critical behavior for $u_->0$ and $B_-<0$. However, for initial positive B_-, the trajectories cannot cross to the $B_-<0$ region and the flows move away from the fixed point. Thus, the shearless model may have renormalized critical exponents, whereas the finite- or infinite-shear models present only first-order ferromagnetic transitions. The corresponding flow diagrams are represented in Fig. 4(a) for $W=0$ and in Fig. 5(a) for $V=0$ by the line linking I_0 [G_0] (Ising [Gaussian]) to I_B [G_B] (renormalized Ising [renormalized Gaussian]).

The complete flow diagram for a general Hamiltonian given by Eqs. (17)–(19) cannot be sketched because the parameter space is fourdimensional (u_-,W,B_-,V), but we may learn about it by means of suitable cuts. The rigid metamagnetic flow diagram of Fig. 3 will serve as a basis to build an overview of the complete diagram. The direction defined by $\delta W=2\delta u_-$ is interesting to study because the RG iterations maintain the trajectories in that same direction. For this particular direction, Eqs. (37) are satisfied by the relations

$$W=W_{GT}=2u_- \quad \text{and} \quad W=W_{IM}=2u_- -\bar{\epsilon}/18. \tag{39}$$

The first condition is represented by the line linking the Gaussian points G_0 and T_V, and the second, by the line connecting the Ising points I_0 and M_V, in the plot of Fig. 3. The flows are always divergent for $W>W_{GT}$. Because the variables u_- and W are independent of B_- and V [see Eq. (37)], this picture remains valid in the space of those fields. W_{GT} and W_{IM} define the subspaces $(W=W_{GT},B_-,V)$ and $(W=W_{IM},B_-,V)$, which contain fixed points of kind $G-T$ and $I-M$, respectively.

We first sketch two-dimensional flow diagrams in Fig. 4. Trajectories in the $(W_{IM},B_-,V=0)$ and $(W_{GT},B_-,V=0)$ planes are presented in Fig. 4(a). Flows in the $(W_{IM},B_-=0,V)$ and $(W_{GT},B_-=0,V)$ planes are shown in Fig. 4(b). The fixed points of the space defined by W_{GT} are into square brackets. Due to the symmetry of the W_{GT} and W_{IM} solutions, which makes the flow diagrams exhibit the same topology, we can draw the two diagrams in the same plot.

From Fig. 4(a) it can be seen that, for $B_-<0$, the Fisher-renormalized fixed points I_B [G_B] and M_0 [T_0] are accessed for $W=0$ and low $W\leqslant W_{GT}$, respectively. As for $B_->0$, the line $B_-=W/2$ (which links I_0 [G_0] to M_B [T_B]) separates two possible behaviors: for $B_->W/2$, the flow is divergent, while for $B_-<W/2$, the runs flow to the Fisher-renormalized Ising [Gaussian] fixed points M_0 [T_0]. The Ising [Gaussian]-like points M_B [T_B] can be accessed only if $W=2B_-$. For the compressible metamagnetic model, the physically accessible

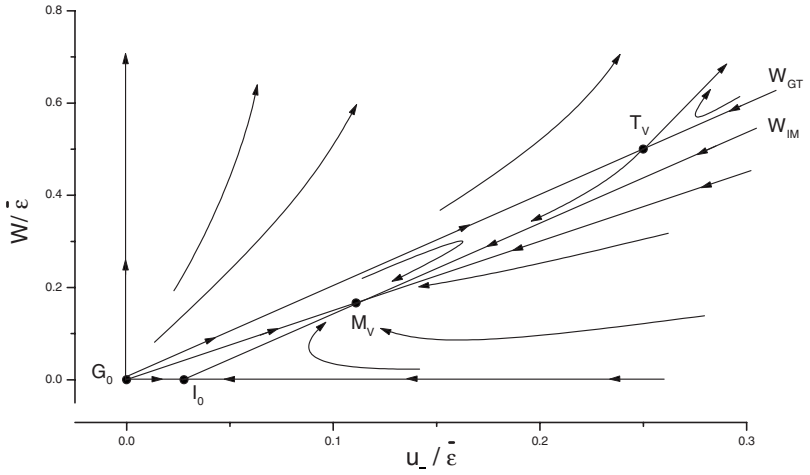

FIG. 3. Flow diagrams for the rigid metamagnetic model ($r_0=r_+$, $V=W$, and $B_-=0$) in the space $W\times u_-$.

region of Fig. 4(a) corresponds to zero magnetic field H and is located on the $(B_->0, W=0)$ segment, where the flow is divergent.

The diagram of Fig. 4(b) is similar to the previous one: for $W<V$, trajectories diverge; for $W=V$, the Ising [Gaussian] M_V $[T_V]$ points are stable; and for $W>V$, the more stable fixed points are again M_0 $[T_0]$ (Fisher-renormalized Ising [Gaussian]). For the metamagnetic model, the physically accessible region of Fig. 4(b) corresponds to null compressibility and is located on the $(V=W>0)$ segment, with the critical behavior of the rigid model, reproduced in Fig. 3.

A more wide-ranging view of the flows can be obtained by drawing three-dimensional diagrams of the trajectories perpendicular to the W axis for $W_{GT}=2u_-$ and $W_{IM}=2u_- -\bar{\epsilon}/18$, for the diagrams of Fig. 4. Top and partial front views of the three-dimensional diagram are shown in Fig. 5. In (a) all the fixed points of Fig. 4 appear. Two diagrams are again overlapped in each figure, with the fixed points of W_{GT} shown in square brackets. Points of the type I $[G]$ are located below the plane of the figure, whereas points M $[T]$ are localized above the plane of the figure. The dashed lines indicate the flows into the plane of points of the type I $[G]$, the continuous lines show the trajectories in the plane of points M $[T]$, dotted lines are some flows among points of the type $I-M$ or $[G-T]$; and dashed-dot lines represent more general flows, indicated by labels.

Analysis of the diagrams shows the relevance of a very special plane, defined by $V=W-2B_-$, where W is W_{IM} or W_{GT}. This surface contains the Ising [Gaussian]-like points I_0 $[G_0]$, I_{VB} $[G_{VB}]$, M_V $[T_V]$, and M_B $[T_B]$. It cuts the plane of

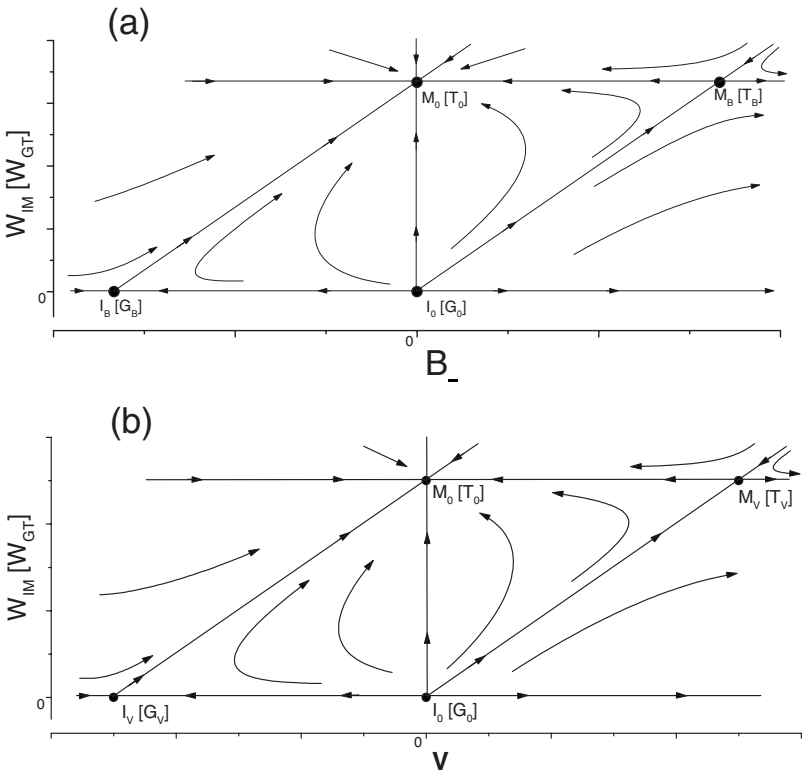

FIG. 4. Flows of the RG that occur at the planes (a) $(W_{IM}[W_{GT}], B_-, V=0)$ and (b) $(W_{IM}[W_{GT}], B_-=0, V)$, where $W_{IM}=2u_- -\bar{\epsilon}/18$ and $W_{GT}=2u_-$. The topology of the trajectories at the subspaces W_{IM} and W_{GT} are identical and can be sketched in the same figure. Fixed points belonging to W_{GT} are written in the square brackets.

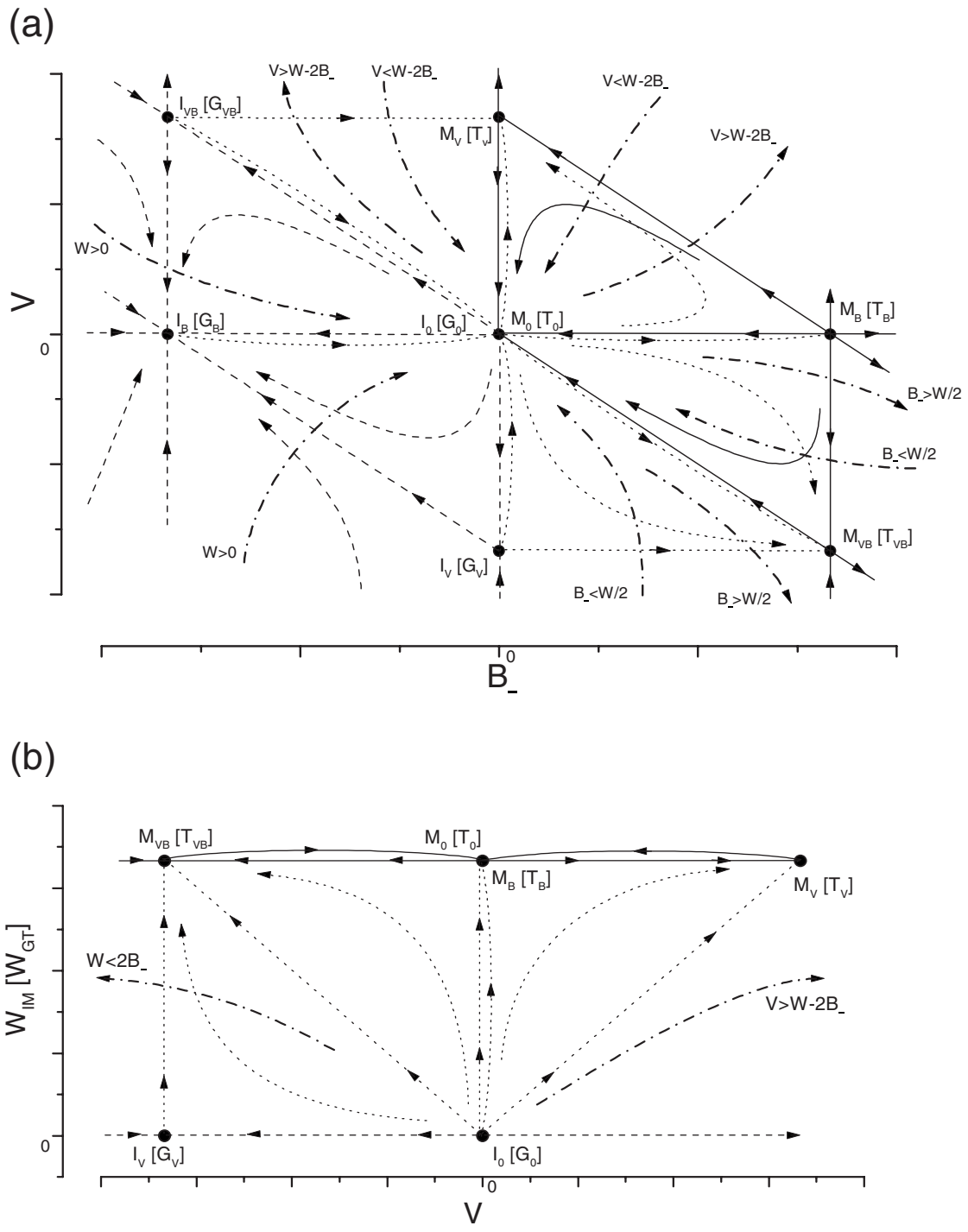

FIG. 5. (a) Top view of the three-dimensional flow diagrams in the subspace $(W_{IM}[W_{GT}], V, B_-)$, i.e., perpendicular to the diagrams of Fig. 4. Dashed lines indicate the flows into the plane of points of type $I[G]$, continuous lines show the trajectories in the plane of points $M[T]$, dotted lines are some flows among points of type $I-M$ and $[G-T]$, dashed-dot lines represent more general flows, indicated by the labels. (b) Frontal view of side $B_->0$ of (a).

Fig. 4(a) at the line linking $I_0\,[G_0]$ to $M_B\,[T_B]$ and the plane of Figs. 4(b) and 5(b) at the line linking $I_0\,[G_0]$ to $M_V\,[T_V]$. This plane separates two different behaviors: in and above it, flows always converge to some fixed point if $W \leqslant W_{GT}$, whereas below this plane the flows are always divergent.

We begin with the analysis of the left side of the figure $(B_-<0)$. The points $I_V\,[G_V]$ and $I_B\,[G_B]$ of the renormalized-Ising [Gaussian] kind and the Ising-like points $I_{VB}\,[G_{VB}]$ and $I_0\,[G_0]$ are in a lower plane, which has $W=0$. These points are accessible only through flows within this plane. The most stable point is renormalized-Ising [Gaussian] $I_B\,[G_B]$, as can be seen by the dashed lines of flows. Above this plane, for $W>0$, there are three regimes: in the region between the $V=W-2B_-$ and the $W=0$ planes, trajectories diverge; in the

$V=W-2B_-$ plane, flows converge to Ising [Gaussian]-like M_V [T_V]; and above the $V=W-2B_-$ plane, trajectories flow to renormalized-Ising [Gaussian] M_0 [T_0].

On the right side of the plot ($B_->0$), in the upper quadrant ($V>0$), the plane $V=W-2B_-$ also separates the RG trajectories. Above it ($V<W-2B_-$), the stable fixed point is again M_0 [T_0] and below it the flows diverge. Within the plane, the most stable point is Ising [Gaussian]-like M_V [T_V], except for the $V=0$ plane, for which also Ising [Gaussian]-like M_B [T_B] becomes the attractor.

Finally, for the lower right quadrant ($B_->0, V<0$), it is the $B_-=W/2$ plane that separates the different flows: above it ($B_-<W/2$), the convergence point is again renormalized-Ising [Gaussian] M_0 [T_0], and below, trajectories diverge. In this plane, the most stable fixed point is Ising [Gaussian]-like M_{VB} [T_{VB}]. A frontal view of the $B_->0$ part of the diagram can be seen in Fig. 5(b).

Outside the subspaces W_{IM} and W_{GT}, the flows have complicated spatial patterns and we shall not try to draw them here. Nevertheless, the general rules stated in the previous diagrams remain valid. For $W>W_{GT}=2u_-$, the flows are always divergent, and if $W<W_{GT}$, the trajectories converge to the subspace defined by W_{IM}, whose flows are represented in Figs. 4 and 5. Therefore, these figures are sufficient to understand the critical behavior of the system.

For the compressible metamagnetic, model both V and B_- are initially positive; thus, the corresponding physical behavior is described by the right upper quadrant of Fig. 5. In this region, the fixed point M_0 (renormalized Ising), to which trajectories head when $W<2u_-$ and $0<V<W-2B_-$, controls the continuous phase transitions. The other accessible fixed points are at the boundaries of the convergence region and are, therefore, all tricritical points. They are Ising-like M_V and M_B if $W=W_{IM}$ and $V=W-2B_-$, renormalized Gaussian-like T_0 if $W=W_{GT}$ and $V<W-2B_-$, and Gaussian-like T_V and T_B at the boundary $W=W_{GT}$ and $V=W-2B_-$. They describe the critical behaviors of particular magnetic systems represented by certain initial Hamiltonians (with specific interaction parameters).

IX. PHASE DIAGRAM FOR THE COMPRESSIBLE METAMAGNET

In order to describe the field-temperature phase diagram, we must analyze the evolution of the critical behavior of the (infinite shear) compressible metamagnet as the magnetic field H increases. The conditions for criticality described in the previous section, $W\leqslant 2u_-$ and $V\leqslant W-2B_-$, may be rewritten in terms of Σ as

$$\frac{2B_-}{\Sigma} \leqslant W \leqslant 2u_-. \tag{40}$$

This inequality relates magnetic field, magnetic interaction constants, and spin-lattice couplings, as we shall see below.

The condition for criticality [Eq. (40)] is not fulfilled at null or small magnetic field H, i.e., small W, and the transition is of first order since the flows diverge.

For finite magnetic field H, three possible behaviors arise:

(1) For low enough $2B_-/\Sigma$, which requires large j_+ and/or a small ratio of ferro- and antiferromagnetic interaction constants J_F/J_A, critical behavior may prevail for intermediary magnetic fields. In this case, the lower limit of Eq. (40) is reached in the $V=W-2B_-$ plane, and the Ising exponent fixed point M_V is accessed. Between the two limits for W, the renormalized-Ising fixed point M_0 is stable. The upper boundary for W turns the renormalized-Gaussian fixed point T_0 stable. Above the upper limit for W, the transition again becomes of first order. The phase diagram, in this case, presents phase coexistence at low and high fields, whereas for intermediate fields the transition is continuous. The line of critical transitions (M_0) is renormalized Ising-like, the low-field tricritical point (M_V) has Ising exponents, and the high-field tricritical point (T_0) has renormalized-Gaussian critical indices.

(2) If the upper and lower limits of the condition given by Eq. (40) approach each other, the line of transition points collapses onto a point on the phase coexistence line. Such behavior is represented by the Gaussian fixed point T_V.

(3) For large $2B_-/\Sigma$, which implies large J_F/J_A, or for $\Sigma<0$, which could result from a "negative" anisotropy of the spin-lattice coupling, the condition for criticality [Eq. (40)] cannot be met, and the transition remains first order for any magnetic field.

Criticality of the model may also be highlighted by noting that, in the reduced Hamiltonian of Eq. (17), with discarded irrelevant variables, the coefficients of the quadratic terms in the spin variables s_0^+ and s_q^+ present no dependence on $\mathbf{q}$. We can, therefore, explicitly integrate over those spin variables. This operation leads to the following reduced Hamiltonian:

$$\Phi_{red} = -\frac{1}{2}\int_{\mathbf{q}} (r_- + \mathbf{q}^2) s_q^- s_{-q}^- + \frac{1}{\Omega}\left(B_- - \frac{W\Sigma}{2}\right)\left(\int_{\mathbf{q}} s_q^- s_{-q}^-\right)^2 - \left(u_- - \frac{W}{2}\right)\int_{\mathbf{q}}\int_{\mathbf{q}'}\int_{\mathbf{q}''} s_q^- s_{q'}^- s_{q''}^- s_{-q-q'-q''}^-. \tag{41}$$

In the absence of compressibility, $r_0=r_+$, $V=W$, and $B_-=0$, the reduced Hamiltonian of the rigid model is recovered.[9] If $V=W=0$, the Hamiltonian for the compressible ferromagnet is obtained.[17,19] The reduced Hamiltonian for the infinite-shear compressible metamagnet has the same general form as that of the compressible ferromagnetic models. Compressibility of ferromagnetic models turns the transition first order, in the cases of finite or infinite shear.[16,17] However, different from the ferromagnetic case, for our infinite-shear metamagnet, the coefficient of the biquadratic term may change sign under the RG transformations, for small magnetic fields, rendering a continuous phase transition possible.

It can be observed that the conditions for the occurrence of the tricritical points ($W=2u_-$ and $V=W-2B_-$) also make one or both of the fourth-order coefficients of the reduced Hamiltonian disappear, resembling a Landau expansion. If both vanish, the last term on the right side of the recursion equation of r_- [Eq. (37)] also vanishes. This term defines the correction of order ϵ to the critical exponent ν, and only in this case do we have a classical (Gaussian) ν exponent, as for the fixed points T_V and T_B.

A final comment on the effect of pressure is as follows. Pressure may decrease lower $2B_-/\Sigma$, and thus, decrease the value of the Ising-like tricritical field. However, within our approach, the $H=0$ transition remains first order.

X. CONCLUSIONS

We have performed a renormalization-group analysis of an infinite-shear compressible metamagnetic model. The procedure consists of a perturbative expansion around the mean-field solution. The RG transformations give rise to 16 fixed points. Flows display two alternative pictures: (i) for low compressibility (or small spin-lattice coupling), the transition line is always first order; (ii) for larger compressibility and in some range of the interaction parameter values, the field-temperature phase diagram may present a second-order transition line at intermediary magnetic fields H. In addition to the low temperature and high field first-order line of the rigid metamagnet, our compressible model may present a second first-order line, at low magnetic field and high temperatures. These two lines join the continuous renormalized-Ising transition line smoothly at tricritical points. The two tricritical points present, respectively, renormalized-Gaussian (at high field) and Ising-like critical exponents (at low field). The length of the critical line depends on the parameters of the system and eventually collapses onto a single point on the coexistence line.

Integrating over the moment independent spin variables of the renormalized Hamiltonian yields a simpler functional, with the same general form as that of the compressible ferromagnetic model. However, unlike the ferromagnetic case, the infinite-shear metamagnetic compressible Ising model can exhibit continuous transitions, because its initially positive biquadratic term may become negative, with increasing magnetic field, for some range of the interaction variables.

We would like to stress the difference between the critical behaviors foreseen by the mean-field and RG calculations. We have shown in previous mean-field calculations[24] that for a small spin-lattice coupling j_+, or equivalently, low compressibility (large elastic constant K), the H vs T phase diagram is the same as that of the rigid model, in which a single tricritical point is present at some intermediary magnetic field H. In that mean-field study,[24] we have also shown, for the special case of isotropic spin-lattice couplings ($j_-=0$), that, for larger j_+ couplings or smaller elastic constant K, there are two possible regimes: (i) a line of continuous transitions may arise at intermediary fields between two tricritical points for small $\frac{J_F}{J_A}$, or (ii) the transition remains first order for any magnetic field if $\frac{J_F}{J_A}$ is large.

The RG study reproduces part of the mean-field predictions. In the first place, a phase diagram equivalent to that of the rigid metamagnet is not possible. Secondly, at null or low fields H, the transition is always first order, independent of interaction parameters. Finally, a second-order transition and two tricritical points may appear for large magnetoelastic coupling or high compressibility and small J_F/J_A. Despite this interesting behavior in the phase diagram, as far as we know, we did not find in the literature any compressible metamagnetic system exhibiting this behavior. According to our calculations, only a metamagnetic system of large compressibility could display this very unusual behavior.

Investigations considering the compressibility with shear forces on systems with $n=1$ ($\alpha>0$) have concluded that it changes the order of the transition.[17] If $n\geqslant 2$ ($\alpha<0$), the transition remains of second order, with the same critical exponents of the rigid model. We have shown that for the metamagnetic model, with $n=1$ in the renormalized Hamiltonian, the compressibility does permit a continuous transition in some range of the interaction parameters.

ACKNOWLEDGMENT

This work was supported by the Brazilian agency CNPq.

APPENDIX A: MEAN-FIELD VARIABLES

The values of $[x_i]$ and y which minimize $\Phi(y,[x_i],T,p,[H_i])$ are obtained by equating to zero the following derivatives of Eq. (4):

$$\frac{\partial\Phi(y,[x_i],T,p,H_k)}{\partial x_k} = -\frac{1}{2}\sum_i x_i L_{ik}^{-1} - \frac{1}{2}\sum_j L_{kj}^{-1}x_j + \tanh(x_k+\beta H_k),$$

$$\frac{\partial\Phi(y,[x_i],T,p,[H_i])}{\partial y} = -y + \frac{1}{2}\sum_{ij} x_i x_j \frac{\partial L_{ij}^{-1}}{\partial y}. \tag{A1}$$

Using Eqs. (3), (6), and (7), we can write

$$\frac{\partial L_{ij}^{-1}}{\partial y} = \frac{1}{N^{3/2}}\sum_{\mathbf{q}} \frac{\tilde{Q}(\mathbf{q})}{\tilde{L}^2(\mathbf{q})}\exp(i\mathbf{q}\cdot\mathbf{\Delta}_{ij}),$$

$$\tilde{Q}(\mathbf{q}) = Q_F\sum_{\nu=2}^{d}\cos q_\nu - Q_A\cos q_1, \quad Q_{F,A} = 2\sqrt{\frac{\beta}{dK}}j_{F,A}. \tag{A2}$$

Using the mean-field coupling (10) and Eqs. (7), (8), and (A2) in Eq. (A1), the mean-field variables can be obtained,

$$-\frac{\tilde{x}(\mathbf{0})}{N\tilde{L}(\mathbf{0})} - \frac{\tilde{x}(\pi\mathbf{1})}{N\tilde{L}(\pi\mathbf{1})}\exp(i\pi k_1) + \tanh(\overline{x_k}+\beta H_k) = 0, \tag{A3}$$

$$\bar{y} = \frac{1}{2N^{3/2}}\left[\frac{\tilde{x}^2(\mathbf{0})}{\tilde{L}^2(\mathbf{0})}\tilde{Q}(0) + \frac{\tilde{x}^2(\pi\mathbf{1})}{\tilde{L}^2(\pi\mathbf{1})}\tilde{Q}(\pi\mathbf{1})\right], \tag{A4}$$

where $\overline{x_k}$ and $\bar{y}$ are the coordinates at the minimum. Note that Eq. (A3) allows only two physical values for $\overline{x_k}$, according to k_1 being even or odd. Looking at Eq. (A3), it can be identified with the mean-field equation of state, as long as the total and staggered magnetizations are

$$m = \frac{\tilde{x}(\mathbf{0})}{N\tilde{L}(\mathbf{0})}, \quad m_s = \frac{\tilde{x}(\pi\mathbf{1})}{N\tilde{L}(\pi\mathbf{1})}. \tag{A5}$$

We still have

$$\overline{x_k} = \tilde{L}(\mathbf{0})m \pm \tilde{L}(\pi\mathbf{1})m_s \quad \text{and} \quad H_k = H \pm H_s, \tag{A6}$$

according to k_1 being even or odd. The mean-field free energy is $-\bar{\Phi}/N\beta$.

APPENDIX B: EXPANDED HAMILTONIAN

1. Hamiltonian in the real space

Substituting $y=\bar{y}+\Delta y$ and $x_i=\overline{x_i}+s_i$ into Eq. (4) and expanding, we get

$$\begin{aligned}\Phi = &-\frac{\bar{y}^2}{2} - \rho_2(\Delta y)^2 - \rho_1 \Delta y - \frac{1}{2}\sum_{i,j}(L_{ij}^{-1})_{\bar{y}}(\overline{x_i x_j} + s_i s_j) \\ &+ \sum_i \ln[2\cosh(z_i)] + \frac{1}{2}\sum_i \cosh^{-2}(z_i)s_i^2 \\ &- \frac{1}{3}\sum_i \cosh^{-2}(z_i)\tanh(z_i)s_i^3 - \frac{1}{12}\sum_i [\cosh^{-4}(z_i) \\ &- 2\cosh^{-2}(z_i)\tanh^2(z_i)]s_i^4,\end{aligned} \tag{B1}$$

where $z_i=\overline{x_i}+\beta H_i$ and

$$\rho_2 = \frac{1}{2}\left[1 + \frac{1}{2}\sum_{i,j}(\overline{x_i}+s_i)\left(\frac{\partial^2 L_{ij}^{-1}}{\partial y^2}\right)_{\bar{y}}(\overline{x_j}+s_j)\right],$$

$$\rho_1 = \frac{1}{2}\sum_{i,j}\left(\frac{\partial L_{ij}^{-1}}{\partial y}\right)_{\bar{y}}(2\overline{x_i}s_j + s_i s_j). \tag{B2}$$

2. Coefficients of Equation (12)

$$\phi_2^+ = \frac{1}{2N}[L^{-1}(\mathbf{q}) - 1 + m^2 + m_s^2], \quad \phi_2^\pm = \frac{mm_s}{N},$$

$$\phi_3^+ = \frac{1}{3N^2}m(1 - m^2 - 3m_s^2), \quad \phi_3^\pm = m_s(1 - 3m^2 - m_s^2),$$

$$\mu_0^+ = \frac{1}{\sqrt{2N\rho_{22}}}\frac{Q(\mathbf{0})}{L(\mathbf{0})}m, \quad \mu_0^- = \frac{1}{\sqrt{2N\rho_{22}}}\frac{Q(\pi\mathbf{1})}{L(\pi\mathbf{1})}m_s,$$

$$\mu_q^+ = \frac{1}{2\sqrt{2}N^{3/2}\sqrt{\rho_{22}}}\frac{Q(\mathbf{q})}{L^2(\mathbf{q})}, \tag{B3}$$

$$\rho_{22} = -1 - \frac{Q^2(\mathbf{0})}{L(\mathbf{0})}m^2 - \frac{Q^2(\pi\mathbf{1})}{L(\pi\mathbf{1})}m_s^2,$$

$$\phi_4^+ = \frac{1}{12N^3}[4(m^2 + m_s^2) - 3(m^4 + 6m^2m_s^2 + m_s^4) - 1],$$

$$\phi_4^\pm = \frac{1}{3N^3}mm_s(2 - 3m^2 + 3m_s^2). \tag{B4}$$

3. Coefficients of Equation (16)

$$r(\mathbf{q}) = [L^{-1}(\mathbf{q}) - 1 + m^2]c_1^{d-1}c_2^2, \quad e = \frac{L^2(\pi\mathbf{1})}{L^2(\mathbf{0})},$$

$$\kappa = 2\left[1 + \frac{Q^2(0)}{L(0)}m^2\right], \quad w = \frac{1}{3}m(1 - m^2)c_1^{2(d-1)}c_2^3,$$

$$u = \frac{1}{96}(1 + 3m^4 - 4m^2)c_1^{3(d-1)}c_2^4. \tag{B5}$$

[1] J. M. Kincaid and E. G. D. Cohen, Phys. Rep., Phys. Lett. **22C**, 57 (1975).
[2] A. F. S. Moreira, W. Figueiredo, and V. B. Henriques, Eur. Phys. J. B **27**, 153 (2002).
[3] D. P. Landau and R. H. Swendsen, Phys. Rev. Lett. **46**, 1437 (1987).
[4] H. J. Herrmann and D. P. Landau, Phys. Rev. B **48**, 239 (1993).
[5] W. Selke, Z. Phys. B: Condens. Matter **101**, 145 (1996).
[6] M. Pleimling and W. Selke, Phys. Rev. B **56**, 8855 (1997).
[7] M. Santos and W. Figueiredo, Phys. Rev. B **58**, 9321 (1998).
[8] M. Zukovic and T. Idogaki, Phys. Rev. B **61**, 50 (2000).
[9] D. R. Nelson and M. E. Fisher, Phys. Rev. B **11**, 1030 (1975).
[10] K. Katsumata, H. A. Katori, S. M. Shapiro, and G. Shirane, Phys. Rev. B **55**, 11466 (1997); Ch. Binek *et al.*, Eur. Phys. J. B **15**, 35 (2000).
[11] W. P. Wolf, Braz. J. Phys. **30**, 794 (2000).
[12] E. Stryjewski and N. Giordano, Adv. Phys. **26**, 487 (1977).
[13] C. Domb, J. Chem. Phys. **25**, 783 (1956).
[14] G. Baker and J. W. Essam, Phys. Rev. Lett. **24**, 447 (1970).
[15] J. Oitmaa and M. N. Barber, J. Phys. C **8**, 3653 (1975).
[16] D. J. Bergman and B. I. Halperin, Phys. Rev. B **13**, 2145 (1976).
[17] J. Bruno and J. Sak, Phys. Rev. B **22**, 3302 (1980).
[18] B. K. Chakrabarti, N. Bhattacharyya, and S. K. Sinha, J. Phys. C **15**, L777 (1982).
[19] V. B. Henriques and S. R. Salinas, J. Phys. C **20**, 2415 (1987).
[20] V. B. Henriques, Ph.D. thesis, Universidade de São Paulo, 1988.
[21] B. Grossmann and D. G. Rancourt, Phys. Rev. B **54**, 12294 (1996); P. Massimino and H. T. Diep, J. Appl. Phys. **87**, 7043 (2000); E. H. Boubcher, P. Massimino, and H. T. Diep, J. Magn. Magn. Mater. **223**, 163 (2001).
[22] S. S. Uda and W. Figueiredo, Phys. Lett. A **117**, 372 (1986).
[23] C. Vettier, H. L. Alberts, and D. Bloch, Phys. Rev. Lett. **31**, 1414 (1973).
[24] A. F. S. Moreira, W. Figueiredo, and V. B. Henriques, Phys. Rev. B **66**, 224425 (2002).
[25] S. Salem-Sugui and W. A. Ortiz, Phys. Rev. B **43**, 5784 (1991).
[26] B. Dunweg and D. P. Landau, Phys. Rev. B **48**, 14182 (1993).
[27] M. Laradji, D. P. Landau, and B. Dunweg, Phys. Rev. B **51**, 4894 (1995).
[28] F. Tavazza, D. P. Landau, and J. Adler, Phys. Rev. B **70**, 184103

(2004).
[29] L. Cannavacciuolo and D. P. Landau, Phys. Rev. B **71**, 134104 (2005).
[30] Xiaoling Zhu, D. P. Landau, and N. S. Branco, Phys. Rev. B **73**, 064115 (2006).
[31] D. P. Landau, Braz. J. Phys. **36**, 640 (2006).
[32] D. J. Amit, *Field Theory, The Renormalization-Group and Critical Phenomena* (McGraw-Hill, New York, 1984).
[33] K. G. Wilson and J. Kogut, Phys. Rep., Phys. Lett. **12**, 75 (1974).
[34] M. E. Fisher, Phys. Rev. **176**, 257 (1968).
[35] A. F. S. Moreira, Ph.D. thesis, Universidade Federal de Santa Catarina, 2003.